

Kristen E. Boyle,¹ Zachary W. Patinkin,¹ Allison L.B. Shapiro,² Peter R. Baker II,³ Dana Dabelea,² and Jacob E. Friedman⁴



Mesenchymal Stem Cells From Infants Born to Obese Mothers Exhibit Greater Potential for Adipogenesis: The Healthy Start BabyBUMP Project



Diabetes 2016;65:647–659 | DOI: 10.2337/db15-0849

Maternal obesity increases the risk for pediatric obesity; however, the molecular mechanisms in human infants remain poorly understood. We hypothesized that mesenchymal stem cells (MSCs) from infants born to obese mothers would demonstrate greater potential for adipogenesis and less potential for myogenesis, driven by differences in β -catenin, a regulator of MSC commitment. MSCs were cultured from the umbilical cords of infants born to normal-weight (prepregnancy [pp] BMI 21.1 ± 0.3 kg/m²; $n = 15$; NW-MSCs) and obese mothers (ppBMI 34.6 ± 1.0 kg/m²; $n = 14$; Ob-MSCs). Upon differentiation, Ob-MSCs exhibit evidence of greater adipogenesis (+30% Oil Red O stain [ORO], +50% peroxisome proliferator-activated receptor (PPAR)- γ protein; $P < 0.05$) compared with NW-MSCs. In undifferentiated cells, total β -catenin protein content was 10% lower and phosphorylated Thr41Ser45/total β -catenin was 25% higher ($P < 0.05$) in Ob-MSCs versus NW-MSCs ($P < 0.05$). Coupled with 25% lower inhibitory phosphorylation of GSK-3 β in Ob-MSCs ($P < 0.05$), these data suggest greater β -catenin degradation in Ob-MSCs. Lithium chloride inhibition of GSK-3 β increased nuclear β -catenin content and normalized nuclear PPAR- γ in Ob-MSCs. Last, ORO in adipogenic differentiating cells was positively correlated with the percent fat mass in infants ($r = 0.475$; $P < 0.05$). These results suggest that altered GSK-3 β / β -catenin signaling in MSCs of infants exposed to maternal obesity may have important consequences for MSC lineage commitment, fetal fat accrual, and offspring obesity risk.

Nearly one in five children in the U.S. is obese (1), and obesity during pregnancy is increasingly recognized as an important contributor to obesity risk in the next generation (2,3). Birth weight and neonatal fat mass are positively associated with maternal BMI (4,5), though neonatal fat-free mass (FFM) is not, suggesting that maternal BMI has a preferential impact on infant adiposity (6). Epidemiological data suggest that these relationships between maternal obesity and offspring adiposity are not confined to neonatal life but affect offspring across the life span, independent of postnatal lifestyle factors (7). However, surprisingly little is known about how maternal obesity might influence obesity risk in the human neonate.

Adipocytes as well as myocytes, osteocytes, and several other cell types all differentiate from the multipotent fetal mesenchymal stem cell (MSC) population. MSC differentiation is regulated by the canonical wingless type (Wnt)/glycogen synthase kinase (GSK)-3 β / β -catenin pathway. In the absence of Wnt signaling, cytosolic β -catenin is constitutively phosphorylated by GSK-3 β , targeting it for proteasomal degradation (8). When activated, Wnt signal transduction leads to sequestration of GSK-3 β , allowing for β -catenin accumulation, nuclear translocation, and initiation of target gene transcription, including myogenic factors such as myogenin (8,9). Alternatively, GSK-3 β inhibitory phosphorylation at Ser9 leads to β -catenin accumulation and nuclear translocation, independent of Wnt signaling (10,11). In vitro studies suggest that β -catenin

¹Section of Nutrition, Department of Pediatrics, University of Colorado School of Medicine, Aurora, CO

²Colorado School of Public Health, Aurora, CO

³Section of Clinical Genetics and Metabolism, Department of Pediatrics, University of Colorado School of Medicine, Aurora, CO

⁴Section of Neonatology, Department of Pediatrics, University of Colorado School of Medicine, Aurora, CO

Corresponding author: Kristen E. Boyle, kristen.boyle@ucdenver.edu.

Received 19 June 2015 and accepted 20 November 2015.

Clinical trial reg. no. NCT02273297, clinicaltrials.gov.

This article contains Supplementary Data online at <http://diabetes.diabetesjournals.org/lookup/suppl/doi:10.2337/db15-0849/-/DC1>.

© 2016 by the American Diabetes Association. Readers may use this article as long as the work is properly cited, the use is educational and not for profit, and the work is not altered.

accumulation can also inhibit adipogenesis via downregulation of CCAAT/enhancer binding protein (C/EBP)- α and peroxisome proliferator-activated receptor (PPAR)- γ (12,13). Studies of pregnant ewes have shown that fetuses exposed to obesity in utero have less skeletal muscle mass, less β -catenin content, and less inhibitory phosphorylation of GSK-3 β , whereas PPAR- γ expression is higher when compared with offspring from control dams (14–16). These data suggest a mechanism whereby maternal obesity could induce a shift in MSC commitment from the myocyte to the adipocyte lineage via disruption of β -catenin signaling. Such a shift in MSC differentiation could have profound effects on fetal tissue development, in particular because there is a large window of overlap for adipogenesis and myogenesis during midgestation, when secondary fetal myogenesis is at its peak (17,18). However, whether this mechanism is evident in MSCs from infants born to mothers with obesity is not known.

We hypothesized that fetal MSCs from infants born to obese mothers would have greater potential for adipogenesis and less potential for myogenesis. Likewise, we hypothesized that differences in the β -catenin pathway could be a potential early determinant of differences in MSC lineage commitment. Last, we investigated whether markers of MSC lineage commitment were correlated with measures of infant body composition at birth.

RESEARCH DESIGN AND METHODS

Ethics Statement

This study used umbilical cord tissue samples and other data collected by the Healthy Start study (R01DK076648, ClinicalTrials.gov identifier NCT02273297). Approval for this study was obtained from the Colorado Multiple Institutional Review Board at the University of Colorado Hospital. Written informed consent was obtained from all participants at enrollment.

Subjects

The Healthy Start longitudinal prebirth cohort study enrolled 1,410 pregnant women, ages 16 and older and at ≤ 23 weeks' gestation, recruited from the obstetrics clinics at the University of Colorado Hospital during 2010–2014. Women were excluded if they had prior diabetes, prior premature birth, serious psychiatric illness, or a current multiple pregnancy. Pregnant women were evaluated twice (at median weeks 17 and 27) for demographics, tobacco use, height, and weight. Fasting blood samples were drawn for measures of glucose, insulin, triglycerides, and free fatty acids (FFAs). Prepregnancy BMI was obtained through medical record abstraction (84%) or self-report at the first research visit (16%). Gestational weight gain was defined as the difference between the mother's prepregnancy weight and her weight at delivery. Infant birth weight was obtained from medical records, and infant weight, length, and body composition (fat mass [FM], FFM; whole-body air

plethysmography [PEA POD; COSMED, Inc.]) were measured within 72 h after birth.

To investigate the biology of intrauterine metabolic programming (BabyBUMP), umbilical cord tissue was obtained at birth from a convenience sample of 165 infants and was used to culture MSCs as part of the ancillary Healthy Start BabyBUMP Project. From this subsample, additionally excluding women younger than 18 years of age upon enrollment and women who developed gestational diabetes mellitus or preeclampsia during the study, 15 obese women (prepregnancy BMI >30 kg/m²) were frequency matched with 15 normal-weight (NW) women (prepregnancy BMI <25 kg/m²) for maternal age, gestational age at delivery, infant sex, and MSC culture time to confluence. During data analysis we discovered that one obese mother had had gestational diabetes mellitus, and this dyad was excluded at that time, leaving 29 dyads for the sample included in this report. Sample selection methods are summarized by flowchart in Supplementary Fig. 1.

MSC Isolation and Culture

MSCs were cultured from fresh umbilical cord tissue explants, as described elsewhere (19) but with slight modification. Briefly, at delivery, a 4-inch section of the umbilical cord was cut below the clamp (infant side) and stored at 4°C in antibiotic-supplemented PBS until processing (≤ 12 h). Umbilical cord tissue explants were dissected free from visible blood vessels and plated, Wharton's jelly side down, onto tissue culture-treated plastic. Low-glucose DMEM supplemented with MSC growth media (Lonza, Walkersville, MD) was added and the explants were maintained at 37°C in 5% CO₂. At confluence, MSCs were harvested for cryogenic storage until experimentation. The number of days to reach cryopreservation (passage 2) was recorded as the culture time to confluence. All experiments were performed on cells in passages 3–4.

Immunophenotype and Cellular Differentiation Analysis by Flow Cytometry

Undifferentiated MSCs were harvested for MSC immunophenotype and CD13/aminopeptidase N (APN) analysis. For all tests, at least 1×10^5 cells were used for staining. All antibodies were titered before the MSC experiments using a pool of primary MSCs and lysed whole blood. For MSC characterization, antibodies (CD73, CD90, CD105, CD34, CD45, and CD19; Supplementary Table 1) were measured in separate aliquots from the same pool of cells (5–10 subjects/pool). This was repeated on four separate pools of cells with mixed representation of MSCs from NW mothers (NW-MSCs) and from obese mothers (Ob-MSCs) (separate experiment days). On each experiment day appropriate IgG isotype controls were measured from the same pool of cells for each fluorescent marker. Mean fluorescence intensity (MFI) was measured for IgG and markers of interest. For CD13/APN expression analysis, MSCs from each subject were tested individually. For

CD13/APN measures, the change in MFI (Δ MFI) was calculated as the difference in MFI from IgG to CD13/APN for all cells.

Adipogenic and myogenic differentiating cells were analyzed by flow cytometry at day 7 of differentiation. Side-scatter area was determined by flow cytometry and compared between undifferentiated and adipogenic differentiating cells as a marker of differentiation induction. Side-scatter signals are largely influenced by the refractive index of intracellular components such as lipids (20). Differentiation efficiency was estimated by the percent of cells positive for BODIPY 493/503 neutral lipid stain (Life Technologies, Carlsbad, CA) at day 7 of adipogenic differentiation and the percent of cells positive for intracellular myogenin protein content at day 7 of myogenic differentiation. These measures were compared between groups in a subset of subjects ($n \geq 5$ per group for all measures). BODIPY 493/503 stain and myogenin antibody were titered before the MSC experiments using a pool of undifferentiated and differentiating MSCs.

Samples were acquired on the Beckman Coulter Gallios Flow Cytometer (Beckman Coulter, Brea, CA) using Kaluza 1.0 data acquisition software. Data were analyzed using Kaluza Analysis 1.3 software. The setup of the flow cytometer is described in Supplementary Table 2. The gating tree was set as follows (Supplementary Fig. 2): light scatter gate (side-scatter area/forward scatter area), live/dead gate (DAPI-negative cells), singlet gate (forward scatter height/forward scatter area). For BODIPY 493/503 and intracellular myogenin measures, cells were fixed before staining; thus the live/dead gate was omitted.

Adipogenic Induction

MSC adipogenesis was induced as described previously (21), with slight modification. Adipogenesis was induced for up to 21 days with three cycles of adipogenic induction medium (low-glucose DMEM, 5% FBS, 1 μ M dexamethasone, 200 μ mol/L indomethacin, 500 μ mol/L 3-isobutyl-1-methylxanthine, 170 pmol/L insulin, and 0.1 \times penicillin/streptomycin [pen/strep]) and adipogenic maintenance medium (low-glucose DMEM, 5% FBS, 170 pmol/L insulin, and 0.1 \times pen/strep) for 3 days each, after which adipogenic maintenance medium was used for the remainder of the experiment. For adipogenesis in the presence of lithium chloride (LiCl), adipogenic induction was performed as described above for 3 days with 10 mmol/L LiCl or without (control) ($n = 9$ per group; from subjects listed in Table 1, matched to remain representative of each group).

Myogenic Induction

MSC myogenesis was induced as described previously (22), with slight modification. MSCs were subcultured on collagen-coated (5 μ g/cm² Collagen I; BD Biosciences, San Jose, CA) dishes, and myogenesis was induced at 90–100% confluence using myogenic induction medium (low-glucose DMEM, 10% FBS, 5% horse serum, 0.1 μ mol/L dexamethasone, 50 μ mol/L hydrocortisone, and 0.1 \times pen/strep) for 7 or 21 days.

RNA Isolation and Analysis

Myosin heavy chain (MyHC) mRNA content was measured from day 0 to day 5 of myogenic induction, as were nanog and Oct4, identified markers of mesenchymal

Table 1—Subject characteristics

	NW (<i>n</i> = 15)	Obese (<i>n</i> = 14)	<i>P</i> value
Maternal characteristics			
Age (years)	28.0 \pm 1.5	26.7 \pm 1.9	0.60
Prepregnancy BMI (kg/m ²)	21.1 \pm 0.3	34.6 \pm 1.0	<0.001*
Primiparous, <i>n</i> (%)	6 (40.0)	6 (42.9)	0.88
Glucose (mg/dL)	74.2 \pm 1.2	76.0 \pm 1.7	0.39
Insulin (μ U/mL)	7.7 \pm 0.5	12.5 \pm 1.7	0.01*
HOMA-insulin resistance	2.1 \pm 0.3	3.1 \pm 0.4	0.07
Triglycerides (mg/dL)	129.3 \pm 15.3	138.7 \pm 12.9	0.64
FFA (mg/dL)	334.9 \pm 28.0	471.8 \pm 44.2	0.01*
Gestational weight gain (kg)	14.2 \pm 0.9	10.2 \pm 2.2	0.10
Gestational age at delivery (weeks)	39.9 \pm 0.2	39.7 \pm 0.3	0.52
Cesarean delivery, <i>n</i> (%)	2 (13.3)	2 (14.3)	0.94
Infant characteristics			
Sex, <i>n</i> (female/male)	7/8	5/9	0.57
Birth weight (g)	3,316.8 \pm 94.7	3,325.9 \pm 102.5	0.95
Birth length (cm)	49.8 \pm 0.5	49.3 \pm 0.5	0.49
FM (g)	270.0 \pm 31.8	358.3 \pm 34.7	0.07
FM (%)	8.43 \pm 0.9	11.1 \pm 0.9	0.05*
FFM (g)	2,877.8 \pm 62.3	2,836.3 \pm 92.8	0.71
FFM (%)	91.6 \pm 0.9	88.9 \pm 0.9	0.05*
MSC characteristics			
Culture time to confluence (days)	26.3 \pm 1.2	26.7 \pm 1.9	0.84

Data are mean \pm SEM, unless otherwise stated. *Significant independent *t* test, $P \leq 0.05$.

stem cell pluripotency (23). Gene names and primer sequences are listed in Supplementary Table 3. Cells were rinsed twice with PBS, then harvested in Buffer RLT (Qiagen, Valencia, CA). Total RNA was isolated using an RNeasy Plus Mini Kit (Qiagen). cDNA was transcribed from 200 ng total RNA using an iScript cDNA Synthesis Kit (Bio-Rad). Quantitative PCR was performed using primer sets for genes of interest, *RPL13a* and ubiquitin C as reference genes, and iQ SYBR Supermix (Bio-Rad, Hercules, CA), as described elsewhere (24). Reactions were run in duplicate on an iQ5 Real-Time PCR Detection System (Bio-Rad), along with a no-template control per gene. RNA expression data were normalized to reference genes using the comparative threshold cycle method.

Lipid Accumulation

Following 21 days of adipogenic induction, cells were rinsed with PBS and fixed with 4% formaldehyde. Cells were stained for 1 h with 0.2% Oil Red O stain (ORO) in propylene glycol, rinsed twice with fresh 85% propylene glycol, then rinsed twice with deionized water. Cellular ORO stain was solubilized with isopropanol for 5 min and transferred to a clean 96-well plate; the degree of staining was determined spectrophotometrically (at 520 nm). Representative photographs were taken using phase-contrast microscopy with a 10 \times objective.

Measures of Protein Content

Cells were rinsed twice with PBS and harvested in cell lysis buffer (CellLytic MT; Sigma-Aldrich, St. Louis, MO) supplemented with protease and phosphatase inhibitor cocktails (Sigma-Aldrich). Subcellular fractionation was performed as described by Abcam. Total protein was determined by bicinchoninic acid assay. Protein content of β -actin, PPAR- γ , fatty acid binding protein (FABP) 4, C/EBP- β , myogenin, MyHC, β -catenin, phosphorylated β -catenin (Thr41/Ser45), phosphorylated β -catenin (Ser552), GSK-3 β , phosphorylated GSK-3 β (Ser9), extracellular signal-related kinases (ERK) 1/2, phosphorylated ERK1/2 (Thr202/Tyr204), phosphorylated Akt (Ser473), phosphorylated signal transducer and activator of transcription 3 (Tyr705), and phosphorylated AMPK (Thr172) were determined by either Western blot as described previously (25) or by simple Western size-based protein assay (ProteinSimple, Santa Clara, CA) following the manufacturer's protocol. Nuclear fractions were used to determine content of β -catenin and PPAR- γ during LiCl experiments, which represent active protein. Results from Western size-based protein assay were analyzed using ProteinSimple Compass software. All antibodies were optimized in house for this system; antibody specifics and assay conditions are listed in Supplementary Table 4.

Statistical Analyses

D'Agostino and Pearson tests were used to assess the normality of the data. Levene tests were used to assess unequal variance. For testing comparisons between

NW-MSCs and Ob-MSCs, independent *t* tests or Mann-Whitney *U* tests were used, where appropriate. For the LiCl experiments, independent *t* tests were used for comparison of NW-MSCs versus Ob-MSCs under control conditions, followed by paired *t* tests for comparison of control versus LiCl conditions for NW-MSCs and Ob-MSCs combined. All data are expressed as mean \pm SEM. Differences between groups were considered statistically significant at $P \leq 0.05$.

Pearson correlations were used to identify relationships between MSC measures. To identify relationships between MSC markers of differentiation and infant body composition, correlation analyses were performed as follows. First, bivariate Pearson correlations were used to identify significant zero-order correlations between infant birth weight, FM (absolute and percent), and FFM (absolute and percent) and MSC measures of ORO staining and FABP4, PPAR- γ , myogenin, and MyHC protein content. Only those factors with significant zero-order correlations between MSC and infant measures were subjected to further analysis; partial correlations were performed with infant sex and maternal prepregnancy BMI included as control variables.

RESULTS

Subject Characteristics

Characteristics for 29 mother–infant pairs included in this substudy are listed in Table 1. By design, the obese mothers had higher BMI but similar maternal age, gestational age at delivery, infant sex, and time to confluence for initial MSC culture. Maternal metabolic markers were measured at a median of 17 weeks' gestation (midpregnancy). At midpregnancy, obese mothers had higher insulin and FFA concentrations ($P < 0.05$) and tended to have higher HOMA-insulin resistance scores ($P = 0.07$), though none of these women had preexisting diabetes or developed gestational diabetes mellitus during the index pregnancy. At birth, compared to the infants of NW mothers, the infants of the obese mothers weighed the same but had higher percent FM and lower percent FFM ($P \leq 0.05$).

Umbilical Cord Cells Express MSC Markers and Differentiate to Adipocytes and Myocytes In Vitro

The umbilical cord cells were >98% positive for staining of MSC markers CD74, CD105, and CD90 and negative for hematopoietic stem cell or lymphocyte markers CD34, CD45, and CD19 (Fig. 1). Adipogenic differentiating cells were increasingly positive for adipogenic markers from day 0 to day 7 (C/EBP- β , PPAR- γ , and ORO stain; Fig. 2A and B), indicating induction of adipogenesis. Side-scatter area increased by 30% from day 0 to day 7 of adipogenesis (Fig. 2C), reflecting a large change in the cellular refractive index. Adipogenic differentiating cells were 97% positive for BODIPY stain at day 7 of differentiation, whereas myogenic differentiating cells were 85% positive for Myogenin Alexa Fluor

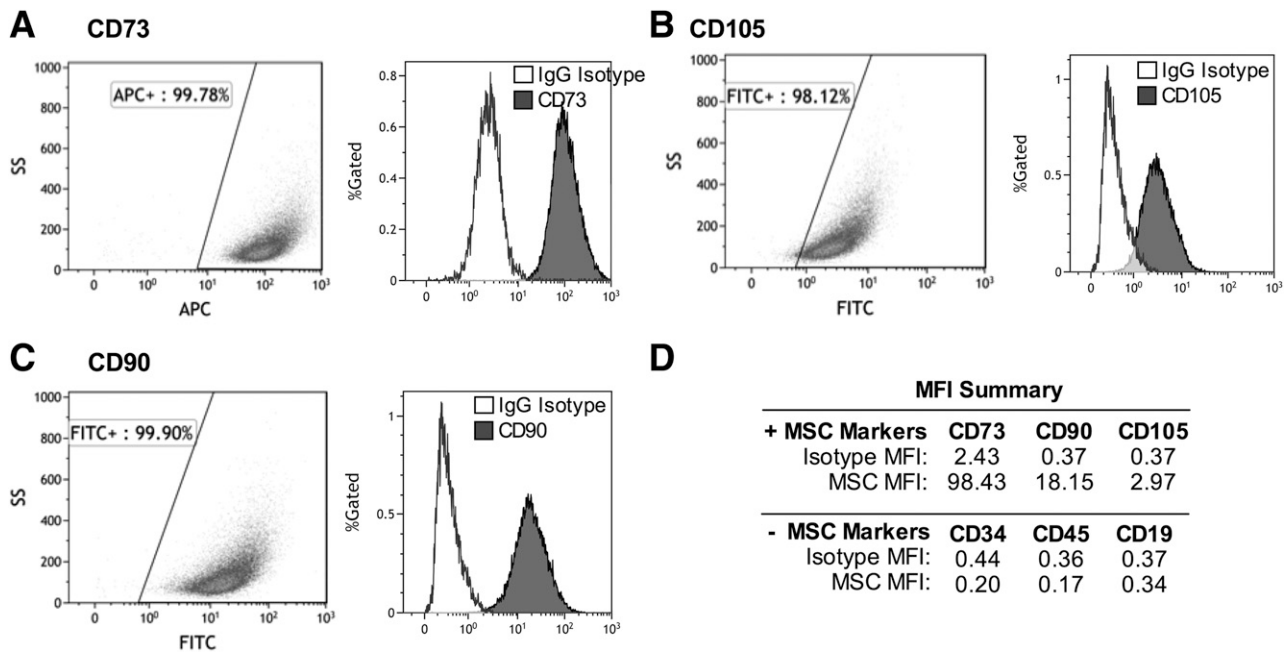


Figure 1—Umbilical cord-derived cells exhibit MSC markers. Undifferentiated cells were pooled (more than five subjects) and stained for MSC markers (CD73, CD105, and CD90) and hematopoietic and lymphocyte markers (CD34, CD45, and CD19). Representative plots are shown for MSC expression of CD73 (A), CD105 (B), and CD90 (C), gated as described in RESEARCH DESIGN AND METHODS. Corresponding histograms show gated cells for IgG isotype controls (white) and the marker of interest (gray). The MFI data summary (D) indicates that cells are positive for MSC markers and negative for hematopoietic and lymphocyte markers. APC, allophycocyanin; FITC, fluorescein isothiocyanate; SS, side scatter.

488 at day 7 of differentiation (Fig. 2D and E). From day 0 to day 5 of myogenesis, cells expressed less of the stem cell markers nanog and Oct4 in mRNA (Fig. 2F and G), whereas mRNA expression of MyHC increased (Fig. 2H). Likewise, from day 0 to day 21 of myogenesis, cells expressed more myogenin and MyHC protein (Fig. 2I), indicating induction of myogenesis. Representative photographs of undifferentiated, adipocyte differentiating, and myocyte differentiating cells show that undifferentiated cells are characteristically spindle-shaped, whereas 21-day adipogenic differentiating cells appear more rounded. Myogenic differentiating cells have begun to fuse together and form tubes (Fig. 2J–L).

Adipogenesis Is Greater in Ob-MSCs, but Markers of Myogenesis Are Not Different

We measured CD13/APN, a potential novel marker of adipogenic potential (26), in undifferentiated cells using flow cytometry. The percent of cells gated at each step was similar for all subjects, indicating no overt differences in cell size, density, or viability (Fig. 3A–C). CD13/APN is a recognized MSC marker and, as expected, >90% of cells were positive for CD13/APN, with no differences observed between groups ($P = 0.80$; Fig. 3D). However, the Δ MFI was over twofold greater in the MSCs from offspring of obese mothers ($P < 0.05$; Fig. 3E and F). Because there were no differences in cell size, density, or viability, or in the number of cells positive for CD13/APN, these data indicate that greater CD13/APN

fluorescence intensity is not the result of differences in cellular morphology or immunophenotype, but represents more cellular protein content.

Once adipogenesis was induced, there were no differences in the percent of cells positive for BODIPY 493/503 neutral lipid stain at day 7 of differentiation ($P = 0.47$; Fig. 4A). At day 3 of adipogenesis, FABP4 protein content was 35% higher ($P \leq 0.05$; Fig. 4B), whereas PPAR- γ protein content was 50% higher ($P \leq 0.05$; Fig. 4C) and ORO staining was 30% higher in Ob-MSCs compared with NW-MSCs at day 21 ($P \leq 0.05$; Fig. 4D and E).

Myogenic differentiating cells were 80–85% positive for myogenin protein at day 7 of differentiation, with no differences between groups ($P = 0.67$; Fig. 4F). Mean group differences in myogenin protein content at day 7 and MyHC protein content at day 21 of myogenesis were consistent, though these results did not reach statistical significance (–16%, $P = 0.14$ and –15%, $P = 0.23$ in Ob-MSCs versus NW-MSCs, respectively, for myogenin and MyHC; Fig. 4G and H). Despite the fact that there were not significant differences in specific myogenic markers, MyHC protein content at day 21 of differentiation was inversely correlated with PPAR- γ protein content in the adipogenic differentiating MSCs ($P < 0.05$; Fig. 4I).

Ob-MSCs Have Less β -Catenin Content and GSK-3 β Inhibitory Phosphorylation

Total β -catenin protein content was 10% lower in undifferentiated Ob-MSCs compared with NW-MSCs, whereas

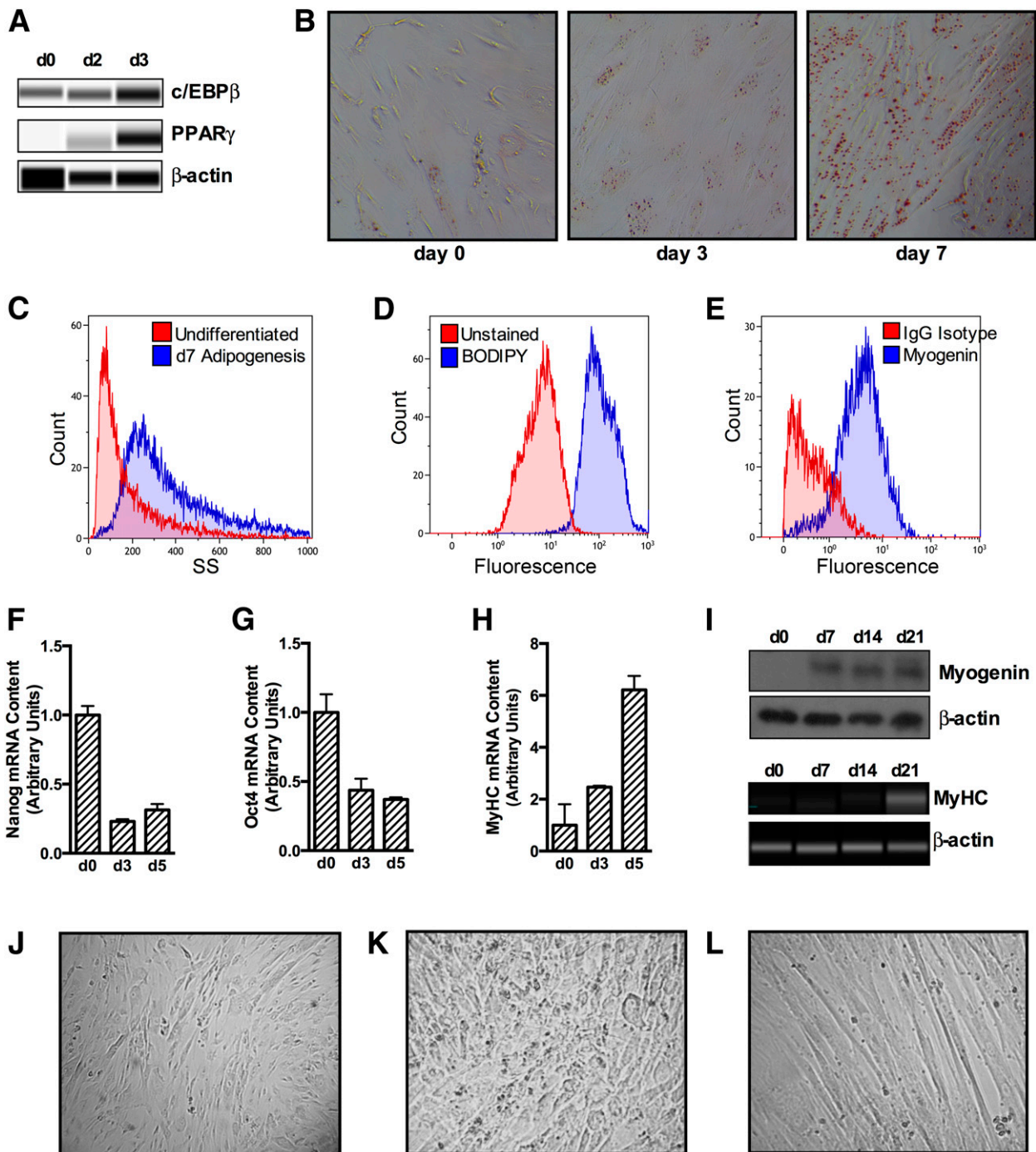


Figure 2—MSCs differentiate to adipocytes and myocytes in culture. Adipogenesis was induced for 2 to 7 days and showed increased protein expression of adipogenic markers c/EBP- β and PPAR- γ (A) and increased ORO staining (B). Side-scatter area increased in adipogenic differentiating cells by day 7 of differentiation (C), and cells were 97% positive for BODIPY 493/503 at day 7 of differentiation (D). Myogenesis was induced for 3–21 days. Cells were 85% positive for myogenin at day 7 of differentiation (E). From day 0 to day 3, cells showed decreased mRNA content of stem cell markers nanog and Oct4 (F and G) and increased mRNA content of the myogenic marker MyHC (H) from days 0 to 5 of myogenic differentiation. Protein content of myogenin and MyHC was increased from 0 to 21 days of myogenesis (I). Representative photographs are shown for undifferentiated (J), 21-day adipogenic differentiating (K), and 21-day myogenic differentiating cells (L). Data are expressed as mean \pm SEM. d, day; SS, side scatter.

phosphorylated/total β -catenin (Thr41/Ser45) was 25% higher ($P < 0.05$; Fig. 5A). Upstream, this corresponded to 25% lower inhibitory phosphorylation of GSK-3 β (phosphorylated Ser9/total) in the Ob-MSCs versus the NW-MSCs

($P < 0.05$; Fig. 5B). There were no difference in stabilizing phosphorylation of β -catenin at Ser552 (1.00 ± 0.07 and 1.07 ± 0.11 in NW-MSCs and Ob-MSCs, respectively; $P = 0.59$) or AMPK phosphorylation at Thr172 (1.00 ± 0.21

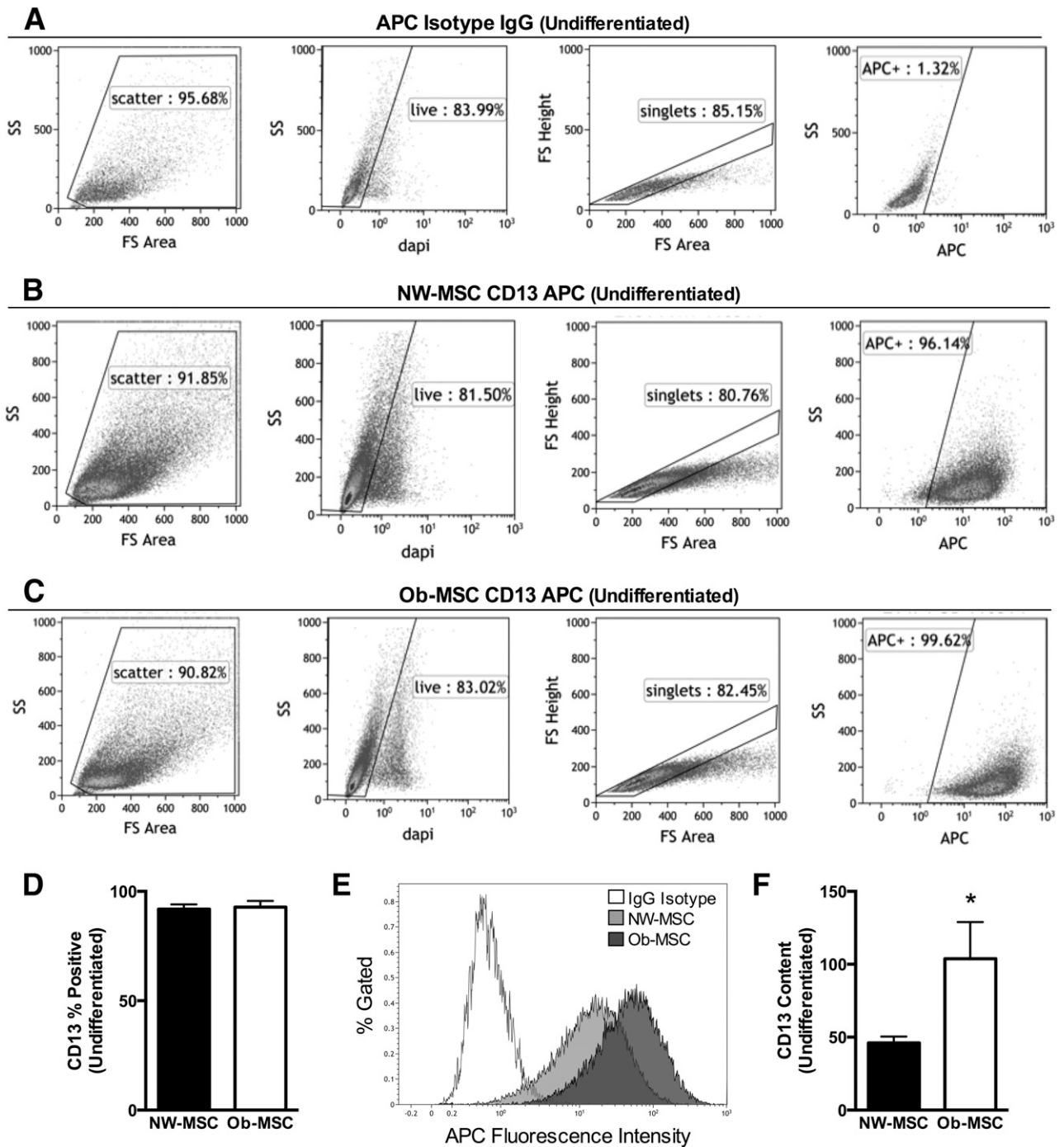


Figure 3—CD13/APN content is greater in Ob-MSCs. Undifferentiated cells from each subject were stained for CD13/APN. Data shown are for the allophycocyanin (APC) IgG isotype control (A) and representative NW-MSC (B) and Ob-MSC (C) flow plots for CD13 APCs. For A–C, graphs are the light scatter gate (first graph), live/dead gate (second graph), singlet gate (third graph), and APC fluorescence intensity (fourth graph) showing that NW-MSCs and Ob-MSCs have similar size, density, and viability. D: The percent of cells positive for CD13/APN was similar for NW-MSCs and Ob-MSCs (black bars and white bars, respectively), though the CD13/APN APC fluorescence intensity, shown from representative subjects (E) and a data summary (F), is higher in Ob-MSCs. Data are expressed as mean ± SEM. *Significant difference from NW-MSCs ($P \leq 0.05$). FS, forward scatter; SS, side scatter.

and 1.06 ± 0.28 in NW-MSCs and Ob-MSCs, respectively; $P = 0.86$), which is shown to phosphorylate β -catenin at Ser552 (27). Phosphorylation of Akt at Ser473, upstream of GSK-3 β , was not different between the groups

(1.00 ± 0.18 and 0.93 ± 0.17 in NW-MSCs and Ob-MSCs, respectively; $P = 0.78$). However, phosphorylated/total ERK1/2 (Thr202/Tyr204) tended to be lower in Ob-MSCs versus NW-MSCs (-20% ; $P = 0.11$; Fig. 5C) and

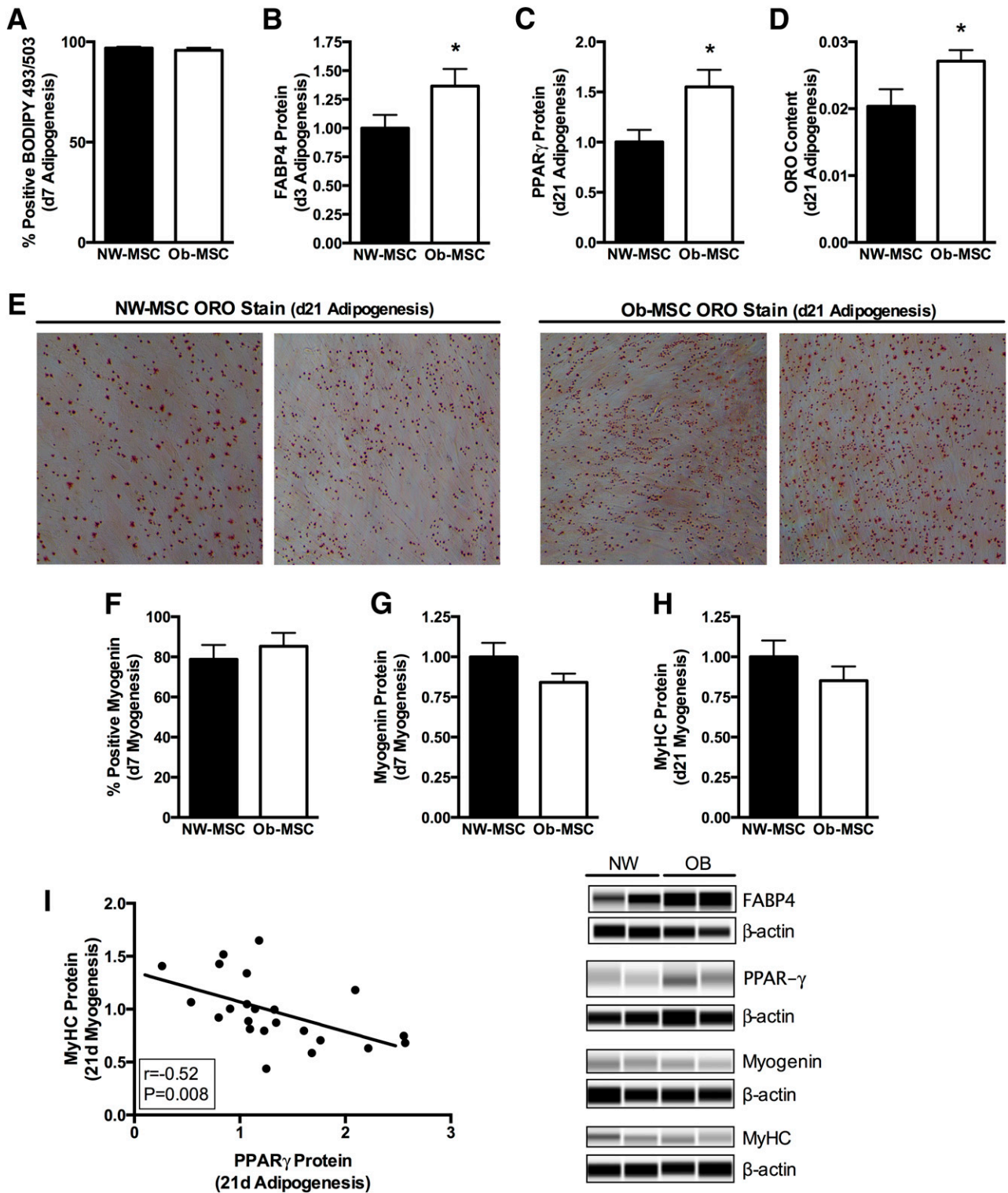


Figure 4—Ob-MSCs exhibit greater potential for adipogenesis but no difference in myogenesis. MSCs from offspring of NW and obese mothers underwent adipogenic or myogenic differentiation for 7 or 21 days, and standard markers were measured. NW-MSCs and Ob-MSCs are black bars and white bars, respectively. At day 7 of adipogenesis, there were no differences in the percent of cells positive for BODIPY 493/503 (A), though the Ob-MSCs expressed more FABP4 (B), PPAR- γ (C), and ORO staining (D) than NW-MSCs at day 21 of adipogenesis. E: Representative photographs of ORO staining at 20 \times magnification are shown for NW-MSCs and Ob-MSCs. At day 7 of myogenesis, there were no differences in the percent of cells positive for myogenin (F) or for total myogenin protein content (G). There were no differences in MyHC at day 21 of myogenesis (H). MyHC protein content in myogenic differentiating cells was inversely correlated with PPAR- γ protein content in adipogenic differentiating cells (I). Data are expressed as mean \pm SEM. *Significant difference from NW-MSCs ($P \leq 0.05$). d, day.

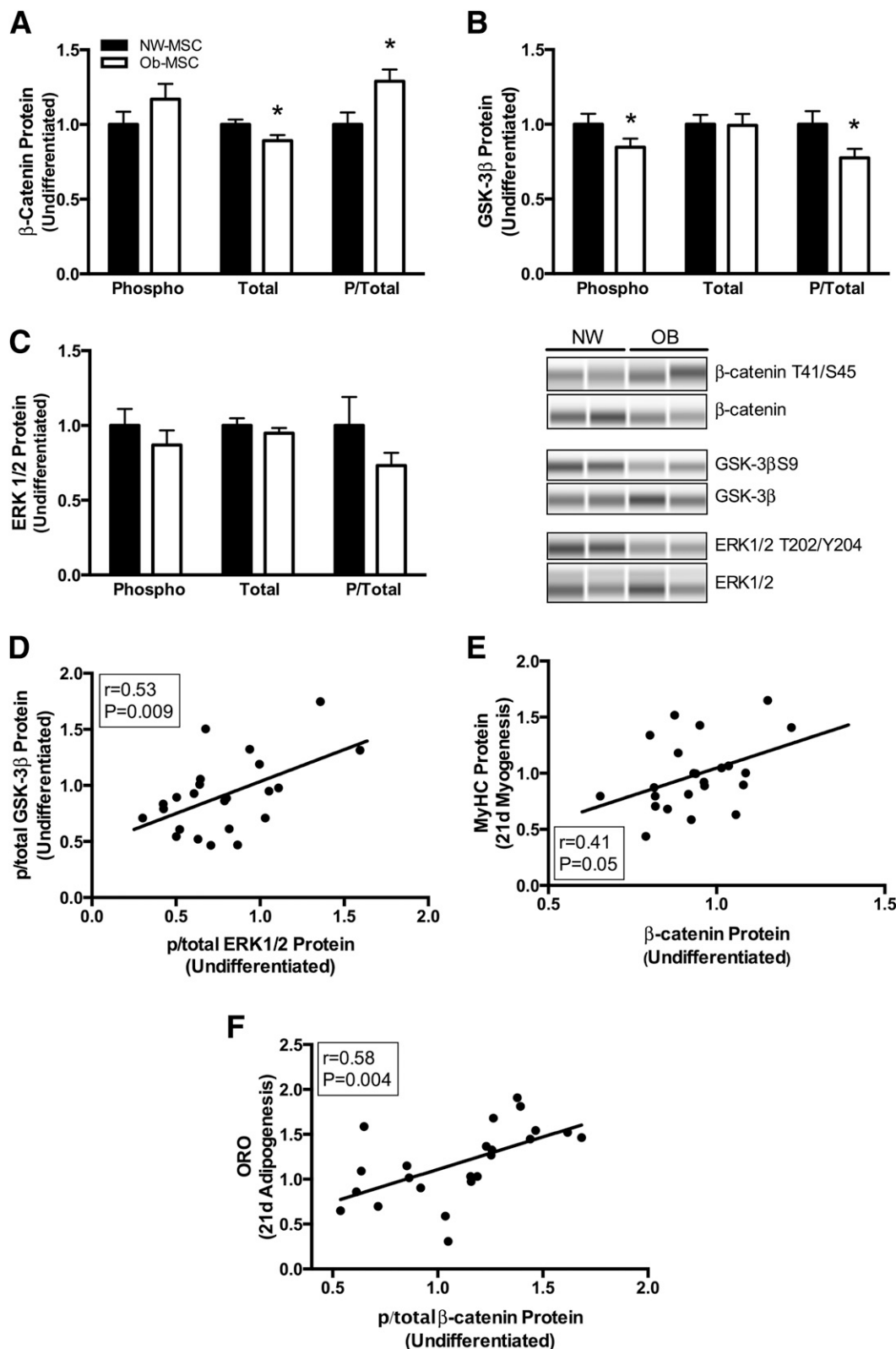


Figure 5—GSK-3β/β-catenin signaling is lower in Ob-MSCs. Amounts of phosphorylated (phospho or P) and total protein was measured in undifferentiated MSCs. **A**: Phosphorylated/total β-catenin (Thr41/Ser45) was increased and total β-catenin content was decreased in Ob-MSCs compared with NW-MSCs (white and black bars, respectively). Upstream of β-catenin, inhibitory Ser9 phosphorylation of GSK-3β was lower in Ob-MSCs, as was phosphorylated/total GSK-3β protein content (**B**). Upstream of GSK-3β, there were no differences in phosphorylated/total ERK1/2 (**C**), though this was correlated with phosphorylated/total GSK-3β (**D**). β-Catenin content in undifferentiated MSCs was positively correlated with MyHC protein content in the 21-day myogenic differentiating cells (**E**), whereas phosphorylated/total β-catenin was correlated with ORO staining in the adipogenic differentiating cells (**F**). Data are expressed as mean ± SEM. *Significant difference from NW-MSCs ($P \leq 0.05$). d, day.

was correlated with GSK-3 β phosphorylation ($P < 0.05$; Fig. 5D). Last, β -catenin protein content was positively correlated with MyHC protein content in the 21-day myogenic differentiating cells ($P < 0.05$; Fig. 5E), whereas phosphorylated/total β -catenin (Thr41/Ser45) was positively correlated with ORO staining ($P < 0.05$; Fig. 5F) and tended to be positively correlated with PPAR- γ protein content (Pearson $r = 0.41$; $P = 0.066$) in 21-day adipogenic differentiating cells.

Inhibition of GSK-3 β Reduces Nuclear PPAR- γ in Ob-MSCs

To investigate the role of GSK-3 β in MSC adipogenesis, we incubated cells with LiCl, a common inhibitor of GSK-3 β . At day 3 of adipogenesis, LiCl increased GSK-3 β phosphorylation and nuclear content of β -catenin ($P < 0.05$; Fig. 6A and B), while reducing nuclear content of PPAR- γ ($P < 0.05$; Fig. 6C). Additionally, nuclear content of β -catenin was lower in Ob-MSCs versus NW-MSCs in the control condition (Fig. 6B).

MSC Adipogenesis Is Correlated With Infant Adiposity

Pearson correlations showed that MSC ORO content in adipogenic differentiating cells was positively correlated with infant FM and percent FM ($P < 0.05$; Table 2). By

nature of the two-compartment body composition measure, MSC ORO was also inversely correlated with percent FFM. The MSC ORO relationships with percent FM and percent FFM remained evident after controlling for maternal prepregnancy BMI and infant sex ($P < 0.05$; Table 2).

DISCUSSION

We have shown that umbilical cord-derived MSCs from babies of obese mothers exhibit greater potential for adipogenesis, as evidenced by larger amounts of three classic markers of adipogenesis. Additionally, we demonstrated that inhibition of GSK-3 β by LiCl led to increased nuclear content of β -catenin and repression of nuclear PPAR- γ protein content. These results are the first evidence that fetal MSCs from infants born to obese mothers exhibit differences in GSK-3 β / β -catenin signaling, including less nuclear content of β -catenin, which may drive subsequent stem cell fate. In addition, we have demonstrated that MSCs' potential for adipogenesis is positively correlated with infant percent FM at birth, suggesting that differences in MSC differentiation may be one mechanism by which babies of obese mothers accrue more fat in utero.

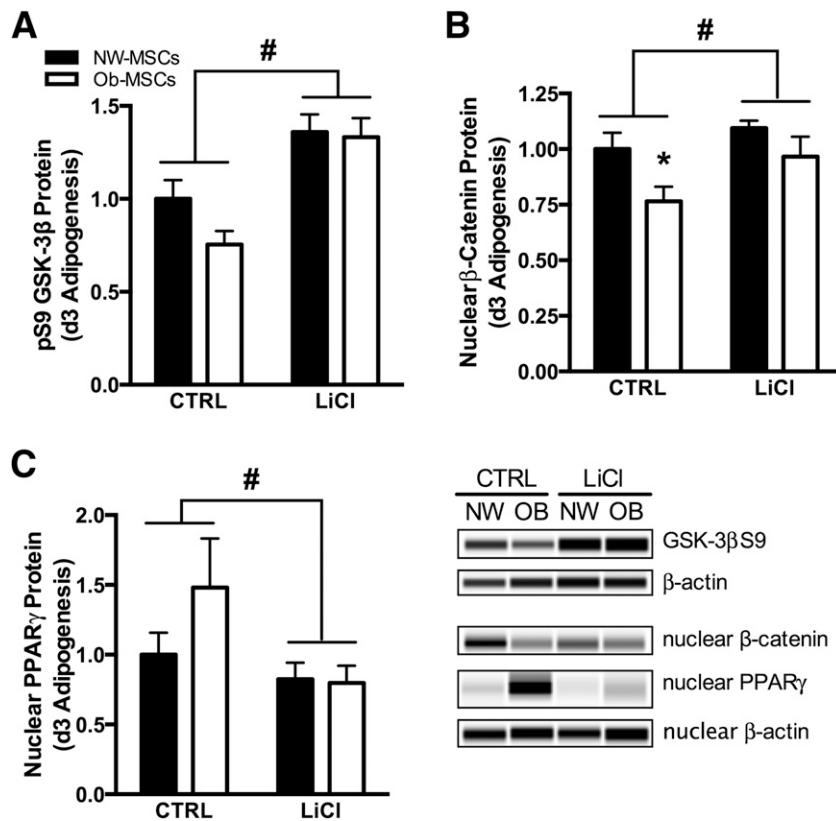


Figure 6—Inhibition of GSK-3 β reduces adipogenesis in Ob-MSCs. MSCs underwent 3 days of adipogenesis with or without LiCl incubation. LiCl induced greater phosphorylation of GSK-3 β in both NW-MSCs and Ob-MSCs (A) and normalized differences in nuclear β -catenin content (B), which represents active protein. Nuclear content of PPAR- γ also was markedly reduced with LiCl incubation (C), indicating lower adipogenic induction. Data are expressed as mean \pm SEM. *Significant difference from NW-MSCs in control (CTRL) conditions ($P \leq 0.05$). #Significant effect of LiCl incubation for NW-MSCs and Ob-MSCs combined ($P \leq 0.05$). OB, obese.

Table 2—Correlations of MSC differentiation markers with infant body composition

	ORO	FABP4	PPAR- γ	Myogenin	MyHC
Bivariate zero-order correlations					
Birth weight (kg)					
<i>r</i>	-0.004	-0.012	0.299	0.330	-0.096
<i>P</i>	0.983	0.966	0.147	0.093	0.633
Birth FM (kg)					
<i>r</i>	0.427	0.259	0.326	0.237	-0.236
<i>P</i>	0.037*	0.351	0.12	0.243	0.247
Birth FM (%)					
<i>r</i>	0.474	0.320	0.249	0.152	-0.221
<i>P</i>	0.019*	0.244	0.241	0.458	0.278
Birth FFM (kg)					
<i>r</i>	-0.045	-0.121	0.303	0.280	-0.061
<i>P</i>	0.833	0.668	0.150	0.167	0.769
Birth FFM (%)					
<i>r</i>	-0.474	-0.320	-0.249	-0.152	0.221
<i>P</i>	0.019*	0.244	0.241	0.458	0.278
Partial correlations†					
Birth FM (kg)					
<i>r</i>	0.402	—	—	—	—
<i>P</i>	0.064	—	—	—	—
Birth FM (%)					
<i>r</i>	0.475	—	—	—	—
<i>P</i>	0.026*	—	—	—	—
Birth FFM (%)					
<i>r</i>	-0.475	—	—	—	—
<i>P</i>	0.026*	—	—	—	—

*Significant result ($P < 0.05$). †Controlled for infant sex and maternal prepregnancy BMI.

β -Catenin signaling induces myogenic differentiation of MSCs (8–10) and also has been shown to inhibit adipogenesis (12,13). In the absence of Wnt signaling, cytosolic β -catenin is constitutively targeted for degradation by GSK-3 β -mediated phosphorylation at several serine/threonine residues. In undifferentiated MSCs we observed greater phosphorylation targeting β -catenin for degradation and less total β -catenin content in Ob-MSCs versus NW-MSCs. We also observed lower inhibitory phosphorylation of GSK-3 β upstream in the Ob-MSCs. Our results are consistent with animal models of maternal obesity, where β -catenin content is 10–15% lower in the fetal skeletal muscle of animals exposed to obesity in utero, as is GSK-3 β phosphorylation (15). It is important to note that Wnt signaling inhibits GSK-3 β by sequestration rather than phosphorylation (10,28). Thus, there are at least *two* mechanisms by which β -catenin accumulation may be regulated: one by Wnt signaling and another by inhibition of GSK-3 β by upstream kinases such as ERK/mitogen-activated protein kinase or Akt (11,29). Indeed, direct inhibition of GSK-3 β reduces adipogenesis and accelerates myogenesis in vitro (30,31). We observed the same effect with regard to adipogenesis when cells were incubated with LiCl, which increased GSK-3 β phosphorylation and nuclear β -catenin content and reduced nuclear content of PPAR- γ , a fundamental regulator of adipogenesis. Upstream, ERK1/2 functions to prime GSK-3 β for inhibitory phosphorylation at Ser9 (31). While we did not

observe differences in the phosphorylation of either Akt or signal transducer and activator of transcription 3, we did observe a trend for lower ERK1/2 phosphorylation in the Ob-MSCs, which was correlated with phosphorylated GSK-3 β . Overall, these data show one mechanism whereby less GSK-3 β phosphorylation in Ob-MSCs could have important consequences for stem cell adipogenesis.

Studies using a sheep model of maternal obesity have linked deficits in β -catenin with poor offspring skeletal muscle development and greater adipogenesis, as evidenced by morphological differences in fetal skeletal muscle tissue from offspring of obese dams (14,15,32). Lower β -catenin content and GSK-3 β phosphorylation in skeletal muscle of these offspring correspond to deficits in MyoD and myogenin protein content, as well as to lower AMPK and Akt phosphorylation and higher PPAR- γ protein content (14,15,32). Although we did not observe statistically significant differences in myogenic markers at either day 7 or day 21 of myogenesis, the 15% deficits in myogenin and MyHC content are consistent in both direction and magnitude with myogenic markers in fetal skeletal muscle from animals exposed to maternal obesity (15). In addition, we did find that MyHC protein content in myogenic differentiating cells was inversely correlated with PPAR- γ content in adipogenic differentiating cells and positively correlated with β -catenin content in undifferentiated cells. Likewise, we found that β -catenin phosphorylation was correlated with lipid accumulation and tended to be correlated with PPAR- γ content in the

adipogenically differentiated cells. Taken together, these relationships suggest that small differences in inherent GSK-3 β / β -catenin signaling in the undifferentiated MSCs may ultimately influence both adipogenic and myogenic pathways.

Our results showing greater adipogenesis in Ob-MSCs versus NW-MSCs are consistent with animal models of adult obesity, where MSCs derived from bone marrow, adipose tissue, or skeletal muscle tissue of genetically obese or streptozotocin-treated rodents exhibit greater adipogenesis compared with MSCs derived from their control counterparts (33–35). Independent of adipogenesis, greater lipid accumulation in the Ob-MSCs may also reflect differences in lipid trafficking or metabolism; regardless of the mechanism, however, greater capacity for adipocyte lipid storage in early postnatal life may be somewhat protective against inflammatory infiltration into adipose tissue depots or “lipid spillover” into other tissues (36).

With regard to maternal obesity and fetal programming events, our results are also consistent with greater adipogenesis in human placental amnion-derived MSCs, where CD13/APN content is elevated and necessary for greater adipogenesis in MSCs from offspring of obese mothers and CD13/APN overexpression is sufficient for inducing greater adipogenesis in MSCs from offspring of NW mothers (26). While CD13/APN is considered a common MSC marker that has been linked to cancer and T-cell proliferation via ERK/mitogen-activated protein kinase signaling (37) and inflammatory and angiogenic mechanisms in vitro (38), very few groups have investigated obesity-related differences in CD13/APN content or function. The contribution of CD13/APN to these processes in vivo or its potential role in stem cell biology remains to be determined.

Maternal obesity increases the risk for neonatal adiposity in humans, independent of diabetic status (4). While circulating maternal glucose and lipid concentrations are associated with neonatal adiposity (6,39), the pathways/mechanisms responsible for greater fetal fat accrual in babies of obese mothers are not well understood. Our study did not address whether the differences we observed in the MSCs were the result of genetic differences passed down from the parents, intrauterine exposure to excess lipids, or other factors associated with the obesity-related milieu. Nevertheless, our results show that MSCs of infants born to obese mothers not only exhibit baseline differences in proteins linked with adipogenesis but also respond more robustly to experimentally induced differentiation, indicating greater inherent propensity for adipogenesis. Experimental inhibition of GSK-3 β revealed that this may be one mechanism for greater adipogenesis in stem cells from infants of obese mothers. Further investigation into the molecular pathways that differ in these cells on the basis of maternal body size, including the potential genetic and epigenetic regulation of these differences, is an important area of future research and

may help us to understand better how obesity during pregnancy increases susceptibility to obesity in the children of these women.

Acknowledgments. The authors thank M. Martinez (the Healthy Start Study project coordinator, Colorado School of Public Health, University of Colorado) and the Healthy Start team for their hard work and dedication. The authors also thank S. Ryan (Department of Pediatrics, University of Colorado School of Medicine) for her assistance with flow cytometry protocols.

Funding. This work was supported by the Obesity Society by an Early Career Research Grant 2013 (to K.E.B.) and the University of Colorado Center for Women’s Health Research by the Junior Faculty Seed Grant (to K.E.B.). Costs for flow cytometry analyses were offset by the National Cancer Institute (Cancer Center Support grant no. P30/CA046934). K.E.B. was supported by the Building Interdisciplinary Research Careers in Women’s Health (BIRCWH) Program from the National Institute of Child Health and Human Development (BIRCWH K12/HD057022, to principal investigator J. Regensteiner). The Healthy Start BabyBUMP Project is supported by grants from the American Heart Association (predoctoral fellowship 14PRE18230008 to A.L.B.S.) and the Colorado Nutrition and Obesity Research Center (National Institute of Diabetes and Digestive and Kidney Diseases grant no. P30 DK048520 to principal investigator J. Hill) and by the parent Healthy Start study (to D.D.). The Healthy Start study was supported by the National Institute of Diabetes and Digestive and Kidney Diseases (R01/DK076648 to D.D.) and the National Institutes of Health/National Center for Advancing Translational Sciences Colorado Clinical and Translational Sciences Award grant no. UL1 TR001082.

Duality of Interest. No potential conflicts of interest relevant to this article were reported.

The contents of this article are the sole responsibility of the authors and do not necessarily represent official NIH views.

Author Contributions. K.E.B. conceived and designed the mesenchymal stem cell study, carried out experiments, analyzed data, and wrote and edited the manuscript. Z.W.P. designed and carried out experiments, analyzed data, and wrote and edited the manuscript. A.L.B.S. carried out experiments and edited the manuscript. P.R.B. assisted with stem cell collection and edited the manuscript. D.D. conceived, designed, and carried out the Healthy Start study and edited the manuscript. J.E.F. designed experiments and edited the manuscript. All authors approved the final version of the manuscript. K.E.B. and D.D. are the guarantors of this work and, as such, had full access to all the data in the study and take responsibility for the integrity of the data and the accuracy of the data analysis.

Prior Presentation. Data from this article were presented at the 75th Scientific Sessions of the American Diabetes Association, Boston, MA, 5–9 June 2015, and at the Obesity Society ObesityWeek, Los Angeles, CA, 4 November 2015.

References

1. Flegal KM, Carroll MD, Kit BK, Ogden CL. Prevalence of obesity and trends in the distribution of body mass index among US adults, 1999–2010. *JAMA* 2012; 307:491–497
2. Gluckman PD, Hanson MA. Developmental and epigenetic pathways to obesity: an evolutionary-developmental perspective. *Int J Obes* 2008;32(Suppl. 7):S62–S71
3. Heerwagen MJR, Miller MR, Barbour LA, Friedman JE. Maternal obesity and fetal metabolic programming: a fertile epigenetic soil. *Am J Physiol Regul Integr Comp Physiol* 2010;299:R711–R722
4. Sewell MF, Huston-Presley L, Super DM, Catalano P. Increased neonatal fat mass, not lean body mass, is associated with maternal obesity. *Am J Obstet Gynecol* 2006;195:1100–1103
5. Starling AP, Brinton JT, Glueck DH, et al. Associations of maternal BMI and gestational weight gain with neonatal adiposity in the Healthy Start study. *Am J Clin Nutr*. 2015;101:302–309
6. Shapiro ALB, Schmiege SJ, Brinton JT, et al. Testing the fuel-mediated hypothesis: maternal insulin resistance and glucose mediate the association

- between maternal and neonatal adiposity, the Healthy Start study. *Diabetologia* 2015;58:937–941
7. Pirkola J, Pouta A, Bloigu A, et al. Risks of overweight and abdominal obesity at age 16 years associated with prenatal exposures to maternal pre-pregnancy overweight and gestational diabetes mellitus. *Diabetes Care* 2010;33:1115–1121
8. von Maltzahn J, Chang NC, Bentzinger CF, Rudnicki MA. Wnt signaling in myogenesis. *Trends Cell Biol* 2012;22:602–609
9. Shang Y-C, Wang S-H, Xiong F, et al. Wnt3a signaling promotes proliferation, myogenic differentiation, and migration of rat bone marrow mesenchymal stem cells. *Acta Pharmacol Sin* 2007;28:1761–1774
10. Armstrong DD, Esser KA. Wnt/beta-catenin signaling activates growth-control genes during overload-induced skeletal muscle hypertrophy. *Am J Physiol Cell Physiol* 2005;289:C853–C859
11. Sharma M, Chuang WW, Sun Z. Phosphatidylinositol 3-kinase/Akt stimulates androgen pathway through GSK3beta inhibition and nuclear beta-catenin accumulation. *J Biol Chem* 2002;277:30935–30941
12. Ross SE, Hemati N, Longo KA, et al. Inhibition of adipogenesis by Wnt signaling. *Science* 2000;289:950–953
13. Kang S, Bennett CN, Gerin I, Rapp LA, Hankenson KD, MacDougald OA. Wnt signaling stimulates osteoblastogenesis of mesenchymal precursors by suppressing CCAAT/enhancer-binding protein alpha and peroxisome proliferator-activated receptor gamma. *J Biol Chem* 2007;282:14515–14524
14. Yan X, Huang Y, Zhao J-X, et al. Maternal obesity-impaired insulin signaling in sheep and induced lipid accumulation and fibrosis in skeletal muscle of offspring. *Biol Reprod* 2011;85:172–178
15. Tong JF, Yan X, Zhu MJ, Ford SP, Nathanielsz PW, Du M. Maternal obesity downregulates myogenesis and beta-catenin signaling in fetal skeletal muscle. *Am J Physiol Endocrinol Metab* 2009;296:E917–E924
16. Zhu MJ, Han B, Tong J, et al. AMP-activated protein kinase signalling pathways are down regulated and skeletal muscle development impaired in fetuses of obese, over-nourished sheep. *J Physiol* 2008;586:2651–2664
17. Barbet JP, Thornell LE, Butler-Browne GS. Immunocytochemical characterisation of two generations of fibers during the development of the human quadriceps muscle. *Mech Dev* 1991;35:3–11
18. Poissonnet CM, Burdi AR, Garn SM. The chronology of adipose tissue appearance and distribution in the human fetus. *Early Hum Dev* 1984;10:1–11
19. Majore I, Moretti P, Stahl F, Hass R, Kasper C. Growth and differentiation properties of mesenchymal stromal cell populations derived from whole human umbilical cord. *Stem Cell Rev* 2011;7:17–31
20. Shapiro HM. Parameters and probes. In *Practical Flow Cytometry*. 3rd ed. Hoboken, NJ, John Wiley & Sons, Inc, 2005, p. 273–410
21. Janderová L, McNeil M, Murrell AN, Mynatt RL, Smith SR. Human mesenchymal stem cells as an in vitro model for human adipogenesis. *Obes Res* 2003;11:65–74
22. Zuk PA, Zhu M, Mizuno H, et al. Multilineage cells from human adipose tissue: implications for cell-based therapies. *Tissue Eng* 2001;7:211–228
23. Tsai C-C, Su P-F, Huang Y-F, Yew T-L, Hung S-C. Oct4 and Nanog directly regulate Dnmt1 to maintain self-renewal and undifferentiated state in mesenchymal stem cells. *Mol Cell* 2012;47:169–182
24. Boyle KE, Newsom SA, Janssen RC, Lappas M, Friedman JE. Skeletal muscle MnSOD, mitochondrial complex II, and SIRT3 enzyme activities are decreased in maternal obesity during human pregnancy and gestational diabetes mellitus. *J Clin Endocrinol Metab* 2013;98:E1601–E1609
25. Boyle KE, Hwang H, Janssen RC, et al. Gestational diabetes is characterized by reduced mitochondrial protein expression and altered calcium signaling proteins in skeletal muscle. *PLoS One* 2014;9:e106872
26. Iaffaldano L, Nardelli C, Raia M, et al. High aminopeptidase N/CD13 levels characterize human amniotic mesenchymal stem cells and drive their increased adipogenic potential in obese women. *Stem Cells Dev* 2013;22:2287–2297
27. Zhao J, Yue W, Zhu MJ, Sreejayan N, Du M. AMP-activated protein kinase (AMPK) cross-talks with canonical Wnt signaling via phosphorylation of beta-catenin at Ser 552. *Biochem Biophys Res Commun* 2010;395:146–151
28. Metcalfe C, Bienz M. Inhibition of GSK3 by Wnt signalling—two contrasting models. *J Cell Sci* 2011;124:3537–3544
29. Bikkavilli RK, Feigin ME, Malbon CC. p38 mitogen-activated protein kinase regulates canonical Wnt-beta-catenin signaling by inactivation of GSK3beta. *J Cell Sci* 2008;121:3598–3607
30. Ohashi K, Nagata Y, Wada E, Zammit PS, Shiozuka M, Matsuda R. Zinc promotes proliferation and activation of myogenic cells via the PI3K/Akt and ERK signaling cascade. *Exp Cell Res* 2015;333:228–237
31. Ding Q, Xia W, Liu J-C, et al. Erk associates with and primes GSK-3beta for its inactivation resulting in upregulation of beta-catenin. *Mol Cell* 2005;19:159–170
32. Zhu MJ, Han B, Tong J, et al. AMP-activated protein kinase signalling pathways are down regulated and skeletal muscle development impaired in fetuses of obese, over-nourished sheep. *J Physiol* 2008;586:2651–2664
33. Vanella L, Sanford C Jr, Kim DH, Abraham NG, Ebraheim N. Oxidative stress and heme oxygenase-1 regulated human mesenchymal stem cells differentiation. *Int J Hypertens* 2012;2012:890671
34. Chuang CC, Yang RS, Tsai KS, Ho FM, Liu SH. Hyperglycemia enhances adipogenic induction of lipid accumulation: involvement of extracellular signal-regulated protein kinase 1/2, phosphoinositide 3-kinase/Akt, and peroxisome proliferator-activated receptor gamma signaling. *Endocrinology* 2007;148:4267–4275
35. Scarda A, Franzin C, Milan G, et al. Increased adipogenic conversion of muscle satellite cells in obese Zucker rats. *Int J Obes* 2010;34:1319–1327
36. Rutkowski JM, Stern JH, Scherer PE. The cell biology of fat expansion. *J Cell Biol* 2015;208:501–512
37. Lendeckel U, Kähne T, Arndt M, Frank K, Ansorge S. Inhibition of alanyl aminopeptidase induces MAP-kinase p42/ERK2 in the human T cell line KARPAS-299. *Biochem Biophys Res Commun* 1998;252:5–9
38. Rahman MM, Ghosh M, Subramani J, Fong G-H, Carlson ME, Shapiro LH. CD13 regulates anchorage and differentiation of the skeletal muscle satellite stem cell population in ischemic injury. *Stem Cells* 2014;32:1564–1577
39. Harmon KA, Gerard L, Jensen DR, et al. Continuous glucose profiles in obese and normal-weight pregnant women on a controlled diet: metabolic determinants of fetal growth. *Diabetes Care* 2011;34:2198–2204